Journal of Control, Automation and Electrical Systems (2019) 30:666–676
https://doi.org/10.1007/s40313-019-00475-w

Time Data-Based Iterative Method for Frequency-Domain Multivariable Systems Identification by Optimized Expansion of Rational Functions

Marcelo A. Oliveira[1] · **Paulo C. Pellanda**[1] · **Roberto Ades**[1] · **Bruno P. Silveira**[2]

Received: 24 October 2018 / Revised: 14 February 2019 / Accepted: 17 May 2019 / Published online: 10 June 2019

Abstract
This paper proposes a deterministic iterative method to obtain a linear time-invariant model of a multivariable plant from time-domain measured data. Model identification is based on frequency response matrices computed from time input–output signals which can be also measured during the normal system operation, possibly without the need of introducing special classes of input signals. Quality of computed frequency response is improved as a new data set is considered at each iteration. The iterative process runs as a filter for noises introduced by system or sensors. Once a frequency response matrix is obtained, a matrix function model is estimated by computing a sequence of optimal and analytical solutions to a convex problem based on a quadratic criterion and an optimized expansion of rational functions. Final identified models are chosen considering a trade-off between small cost and low complexity (small order). Numerical examples are used to evidence advantages and limitations of the method.

Keywords Multivariable systems identification · Fast Fourier transform · Frequency response · Optimized expansion of rational functions

1 Introduction

Mathematical models of dynamic systems are particularly useful for both theoretical and numerical analysis and synthesis of control systems. Closed-loop control is commonly used to modify the system behavior to meet robustness requirements for stability and performance. An adequately tuned model is often able to represent the system dynamics satisfactorily without presenting excessive mathematical complexity to allow applying advanced control system methods. A natural way to obtain differential equations to model system dynamics is by using dynamic analysis based on physical principals. System identification is an alternative to that class of modeling techniques which, in some cases, can be impractical or difficult due to the complexity of physical laws describing the system dynamics (Tóth 2010).

Several approaches have been presented to address the problem of identifying systems in the frequency domain, and there is currently a large literature available on this subject; see Ljung (1999), Pintelon and Schoukens (2012), Tischler and Remple (2012) and Ljung (2013), for instance. In Ljung (2013), an overview about identification of linear systems is presented. It covers the classical approach of parametric methods by means of maximum likelihood and prediction error methods, as well as some classical nonparametric methods through spectral analysis. Some approaches are based on least square method (Sanathanan and Koerner 1963; Drmac et al. 2015; Galrinho 2016). Other studies use H_∞-norm-based estimation (Ninness 1998; Vizer 2015). It is also observed that some works propose two-stage algorithms (Akçay and Heuberger 2001): an estimation of a high-order model is performed before the application of a model order reduction technique, normally based on balanced truncation

✉ Marcelo A. Oliveira
oliveira.marcelo@ime.eb.br

Paulo C. Pellanda
pellanda@ime.eb.br

Roberto Ades
rades@ime.eb.br

Bruno P. Silveira
bpinhosilveira@yahoo.com.br

[1] Defense Engineering Graduate Program, Military Institute of Engineering, Rio de Janeiro, Brazil

[2] Universidade de las Fuerzas Armadas, Sangolqui, Ecuador

theory. In (Ninness 1996; Oliveira et al. 2011), orthonormal basis functions such as Laguerre or Kautz are used for series expansion of rational transfer functions. In general, the main concern is to solve the identification problem as a solution to a convex optimization problem.

Despite frequency identification techniques are widely used in practice, in certain cases, especially in highly complex systems, their application may be difficult or even impractical, notably due to the impossibility of exciting the system with specific classes of signals having sufficient high amplitudes. It is also worth mentioning that, in some situations, it is also difficult to interfere with (or make the necessary field tests during) the system regular operation. Identification of electromechanical dynamics in large hydroelectric power plants is a typical example where there are difficulties in obtaining field data from the power machines operating in closed loop and regularly connected with the rest of the system due to the associated risks (Bossa et al. 2011). In addition, the system could be unstable in open loop or not contain important oscillation modes if some generators are not synchronized with the rest of the system during field tests.

In this paper, a three-step method of frequency-domain identification of a multiple-input multiple-output (MIMO) system based on a convex optimization problem is presented. In the first one, a frequency response matrix (FRM) is iteratively computed, considering a particular bandwidth of interest, from simultaneous measurement of system inputs and outputs. The idea in this first step is to also consider the possibility of interfering minimally on the normal system operation. That is, no specific classes of exciting inputs must necessarily be considered provided that the regular operating (input/output) signals are rich enough. If this does not occur, in systems whose inputs are excitable for model identification purposes, some specific signals can be used, such as the swept sine, also called periodic chirp, Schroeder multisine, which is a sum of harmonically related sine waves, and the pseudorandom binary sequence (Pintelon and Schoukens 2012). Then, an alternative approach is based on the principle of superposition. That is, these specific signals can be added to the operating system inputs as disturbances with small amplitudes, interfering minimally in its operation, as in the large power plant example reported by Bossa et al. (2011). In a second step of the method, for a set of previously chosen orders, $\{n\} \in \mathbb{N}^+$, a corresponding family of n^{th}-order rational and proper models, $G_e^n(s)$, is estimated by computing a sequence of optimal solutions to a convex problem based on a quadratic criterion. The best model is chosen considering a trade-off between small cost and low complexity (small n). Finally, in the last step, the identified model is validated.

2 Proposed Method

2.1 General Problem Statement

Consider a linear time invariant (LTI) MIMO system with p inputs and q outputs and a given set of time-domain sampled input/output data. The general black box identification problem (Ljung 1999; Pintelon and Schoukens 2012) in the frequency domain to be solved can be stated as follows: *determine a transfer function matrix (TFM) model, $G_e(\underline{\theta}, s)$, with limited and reduced complexity whose frequency response be as close as possible to that of the system, according to a given optimization criterion.* In this case, limited and reduced complexity means that the estimated model depends on a real parameter vector, $\underline{\theta}$, of finite and reduced dimension. The system to be identified can be nonlinear since the available small-signal data are obtained from field tests performed on a stable operating point.

2.2 General Algorithm

The identification method is proposed to be performed in three main steps as shown in the algorithm of Fig. 1. A frequency response is first determined from measured time data

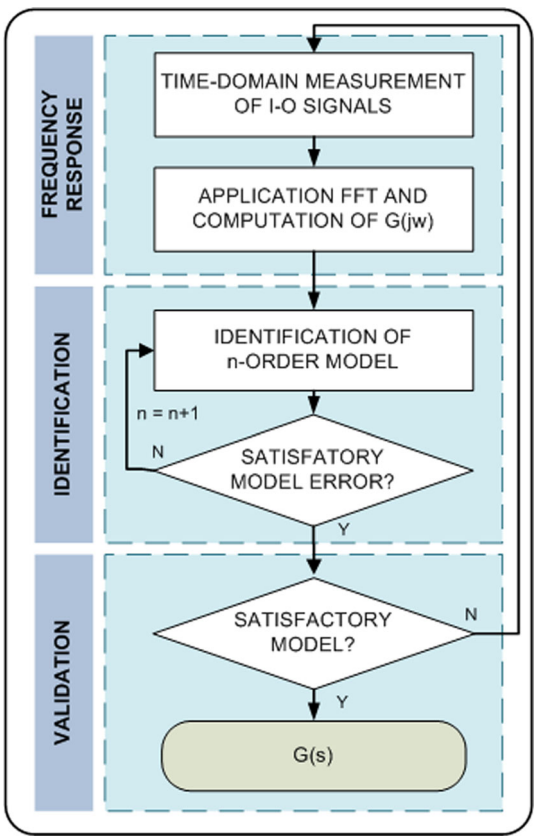

Fig. 1 Proposed general algorithm

considering a bandwidth of interest (first step described in Sect. 2.3). Then, an n-order TFM model is tuned by using a basis expansion that minimizes an optimal quadratic norm (second step described in Sect. 2.4). The estimated model order n is iteratively increased up to a previously established cost is reached, which results in a corresponding family of models of different orders. The choice of the most appropriate order n and hence $G_e^n(s)$ is based on a trade-off between the precision required to represent the dynamic behavior of the plant and the mathematical complexity of the model. Once an n-order system model has been estimated, it can be validated by using some algorithm, e.g., one of the methods presented by Ljung (1999). If the validation fails, the overall identification process has to be restarted by using a new set of measured data. Regarding the computational burden, it is mainly related to the application of the fast Fourier transform (FFT) in the first step and with the solution of two system of linear equations (SLE), in the first and second. In fact, the algorithm is polynomial time in general: in the first step, it is $\mathcal{O}(p^3)$, $\mathcal{O}(q)$ and $\mathcal{O}(m)$, where m is the dimension of the frequency vector; in the second step, it is $\mathcal{O}(n^3)$, $\mathcal{O}(p)$, $\mathcal{O}(q)$ and $\mathcal{O}(m)$.

2.3 Obtaining Frequency Response Data

According to Schumacher et al. (2015), frequency-domain data can be obtained in three ways: as a solution to a non-parametric identification problem in which an estimate of the frequency response of the system is computed from time-domain input/output data; through the application of the FFT to the time-domain input/output data; and by a direct measurement of the frequency response of the system. Here, we propose to apply the FFT to time data. The frequency response of each plant channel is obtained through the solution of an SLE. For multiple-input single-output (MISO) and MIMO cases, the idea is to split each set of sampled input/output data into a family of windows not necessarily having the same number of points. Each window corresponds to one equation in the SLE. Then the number of windows must be equal to (or greater than) the number of inputs so that an (over)determinate SLE is obtained, as detailed in the following sections. A sequence of iterative solutions is then computed for each new set of time data until a smooth and rich frequency response is obtained. That is, the effect of noises and outliers in measured time data is attenuated and more frequency components are introduced in the frequency response as the number of iterations increases.

2.3.1 SISO Case

The classical procedure to obtain a frequency response of a stable LTI single-input single-output (SISO) system is based on the fact that, if it is subjected to a sinusoidal input, its output will, at steady state, be a sinusoidal signal of the same frequency as the input, but with different amplitude and phase. Thus, it is enough to excite the system with sinusoidal inputs having frequencies in a range of interest to obtain a discrete number of frequency data. However, this procedure may present some practical difficulties. For instance, it is not always possible to excite a system with specific classes of signals. Besides, for same complex systems like chemical processes, for example, time spent in this kind of test may be prohibitive due to very slow dynamics involved.

An alternative to the aforementioned procedure is to apply the FFT to the input and output plant signals measured during regular operation conditions, as indicated in the first step of Fig. 1, considering or not some additional small disturbance inputs. For SISO systems, the frequency response curves can be computed by sampling input and output signals and applying the FFT to $u(kT)$ and $y(kT)$, where $k \in \{1, 2, \ldots\}$ and T is the sampling time (Ljung 1999; Pintelon and Schoukens 2012; Tischler and Remple 2012):

$$G(j\omega_i) = \frac{Y(j\omega_i)}{U(j\omega_i)}, i \in \{1, 2, \ldots, m\}, \tag{1}$$

where $U(j\underline{\omega}) = \text{FFT}[u(kT)]$, $Y(j\underline{\omega}) = \text{FFT}[y(kT)]$ and $\underline{\omega} \in \mathbb{R}^m$ is a frequency vector.

2.3.2 MISO Case

For MISO systems, with p inputs and for $i \in \{1, \ldots, m\}$, the output in the frequency domain can be written as:

$$\begin{aligned} Y(j\omega_i) = {} & G_{11}(j\omega_i)U_1(j\omega_i) + G_{12}(j\omega_i)U_2(j\omega_i) \\ & + \cdots + G_{1p}(j\omega_i)U_p(j\omega_i). \end{aligned} \tag{2}$$

In this case, computing all entries of $G(j\omega_i)$ simultaneously by using relation (1) is not possible due to multiplicity of inputs. To overcome this problem, one can take advantage of the superposition property of linear systems by testing each input–output pair independently (and alternately) which can be costly in terms of time spent in the process. Besides, that maneuver could be infeasible for financial, operational or technical reasons in an industrial plant, for instance.

A practical way proposed here to compute all entries of $G(j\omega_i)$ simultaneously is by splitting a set of input–output samples into subsets (windows), not necessarily containing the same number of points, and constructing a set of linear equations whose unknown variables are the coefficients $G_{1k}(j\omega_i)$, $k \in \{1, 2, \ldots, p\}$. The number of windows must be equal to (or greater than) the number of inputs so that an (over)determinate system of linear equations is obtained. This allows determining a system frequency response for a selected set of discrete frequencies. This computation is repeated as many times as needed so that, by monitoring the

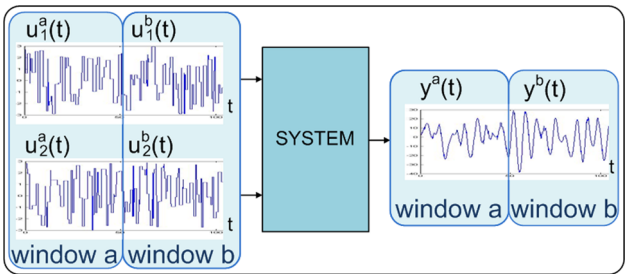

Fig. 2 Two-input two-window case

system inputs and the output, the frequency response converge iteratively to a solution.

Consider now, for instance, the case of a two-input system and data split into two windows, a and b, as illustrated in Fig. 2. For a vector of m selected frequencies, the following set of linear equations is obtained, where $i \in \{1, 2, \ldots, m\}$ (Oliveira et al. 2017):

$$\begin{cases} G_{11}(j\omega_i)U_1^a(j\omega_i) + G_{12}(j\omega_i)U_2^a(j\omega_i) = Y^a(j\omega_i), \\ G_{11}(j\omega_i)U_1^b(j\omega_i) + G_{12}(j\omega_i)U_2^b(j\omega_i) = Y^b(j\omega_i). \end{cases} \quad (3)$$

For a given frequency value, problem (3) defines an SLE which may be undetermined if the associated (2×2)-matrix is singular or poorly conditioned. A condition to be satisfied such that this problem is well conditioned is that the input frequency spectra vary sufficiently from one window to another. Otherwise, SLE (3) will be almost linearly dependent. If this is the case, a good practice is to consider a greater period of time for data measurements to get rid of singularities, since it is enough that small variations occur at least in one of the inputs from window a to b for a given frequency range of interest $\omega \in [\omega_1,\ \omega_m]$.

Notice that SLE (3) can be rewritten as a single system of linear equations as follows:

$$\begin{bmatrix} \mathcal{U}_1 & 0 & \cdots & 0 \\ 0 & \mathcal{U}_2 & \cdots & 0 \\ \vdots & \vdots & \ddots & \vdots \\ 0 & 0 & \cdots & \mathcal{U}_m \end{bmatrix} \begin{bmatrix} \mathcal{G}_1 \\ \mathcal{G}_2 \\ \vdots \\ \mathcal{G}_m \end{bmatrix} = \begin{bmatrix} \mathcal{Y}_1 \\ \mathcal{Y}_2 \\ \vdots \\ \mathcal{Y}_m \end{bmatrix}, \text{ where} \quad (4)$$

$$\mathcal{U}_i = \begin{bmatrix} U_1^a(j\omega_i) & U_2^a(j\omega_i) \\ U_1^b(j\omega_i) & U_2^b(j\omega_i) \end{bmatrix}, \quad \mathcal{G}_i = \begin{bmatrix} G_{11}(j\omega_i) \\ G_{12}(j\omega_i) \end{bmatrix}, \quad \mathcal{Y}_i = \begin{bmatrix} Y_1^a(j\omega_i) \\ Y_1^b(j\omega_i) \end{bmatrix}$$

and $i \in \{1, 2, \ldots, m\}$.

From now on, the first step of algorithm in Fig. 1 is more deeply studied and detailed for the MISO case, as shown in Fig. 3. This new algorithm has four main parts. First two parts basically consist of obtaining a three-dimensional matrix with the data related to the system input/output frequency spectra, computed from time-domain measured signals. Last two parts define and solve iteratively a set of SLE. The resulting FRM is computed as an average of all iterative solutions. Algorithm in Fig. 3 can be described by the following steps:

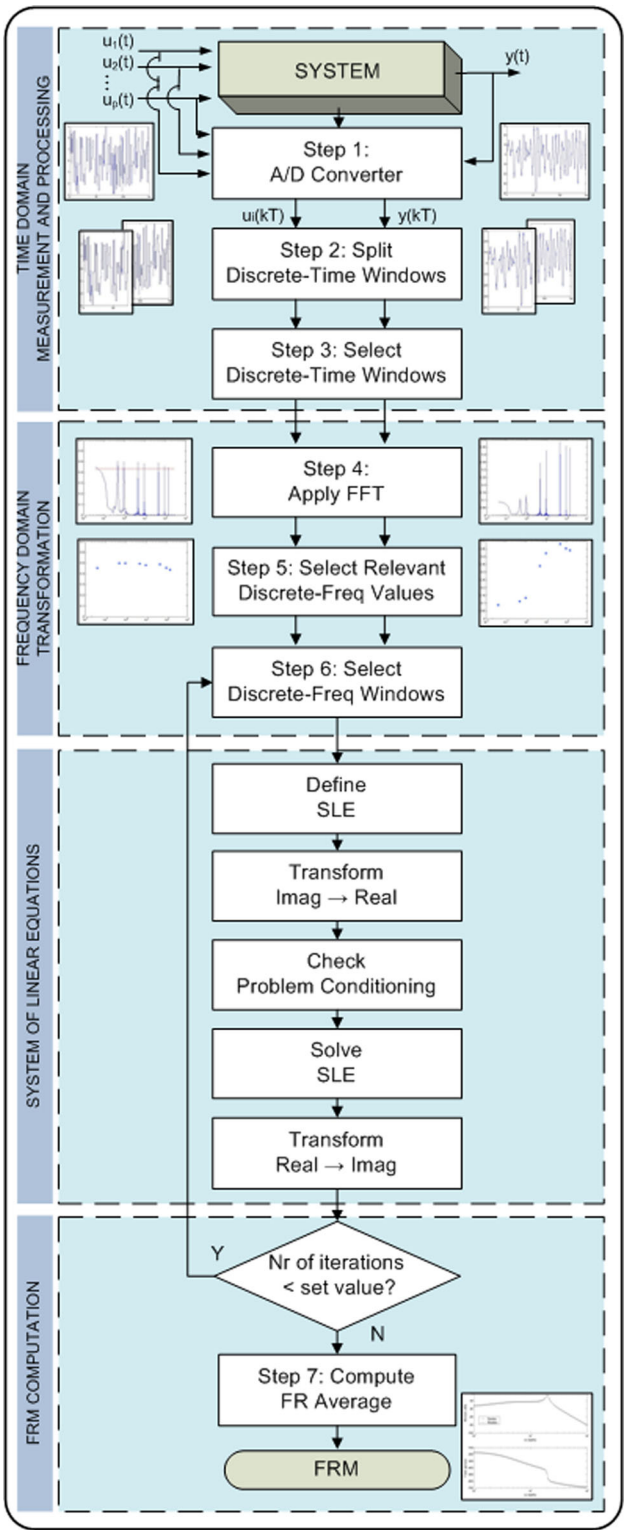

Fig. 3 FRM computation—MISO system case

Algorithm 1 : FRM computation for MISO systems

Step 1: *Measure discrete-time input/output data by using a sampling rate T suitably chosen to capture main system dynamic features in terms of frequency spectra.*

Step 2: *Split sampled input/output data into a family of discrete-time windows not necessarily having the same number of points. The data windows are arranged and stored as pages (or cards) in a three-dimensional (3D) matrix as shown in Fig. 4.*

Step 3: *Analyze each page to select those whose input variation rates are high enough to excite system dynamics. Hence cards containing smooth input sequences with variation rates below a predefined tolerance are discarded.*

Step 4: *Apply FFT to matrix columns of each page to obtain a new 3D matrix of input and output frequency spectra. In each new card, the time vector column is replaced by another of linearly spaced frequencies. New remaining columns will correspond to the associated input or output vectors in the frequency domain.*

Step 5: *Select discrete-frequency values for which the corresponding frequency-domain input values are relevant in order to reduce the computational burden. The following selection criteria can be used either in a separately or jointly way: select points of maxima, above a specified cutting threshold and/or above a cutting threshold proportional to the signal average.*

Step 6: *Iteratively solve the problem of computing FRM by selecting and processing a number of discrete-frequency pages in a sequential or a random way. For each iteration, define and solve an SLE with at least as many equations (pages) as the number of system inputs, as in (4). It should be noted that the coefficients of SLE (3) are complex numbers. We efficiently solve complex SLE by using numerical algorithms presented in (Militaru and Popa 2012). The basic idea is to transform the given complex system into a real one and solve the problem by the direct method (Strang 2006). If SLE in (4) is poorly conditioned for a given frequency value ω_i, it is discarded.*

Step 7: *The procedure is repeated until the number of iterations reaches a predetermined maximum value. FRM entries are obtained by computing their average values for each selected frequency, considering the total number of iterations.*

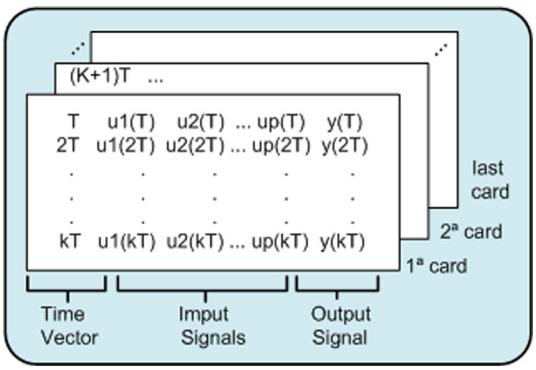

Fig. 4 Discrete-time input/output data stored as a family of windows in a 3D matrix

2.3.3 MIMO Case

For MIMO systems with p inputs and q outputs, equation (2) becomes:

$$\begin{aligned} U_1(j\omega_i)G_{11}(j\omega_i) + \ldots + U_p(j\omega_i)G_{1p}(j\omega_i) &= Y_1(j\omega_i), \\ U_1(j\omega_i)G_{21}(j\omega_i) + \ldots + U_p(j\omega_i)G_{2p}(j\omega_i) &= Y_2(j\omega_i), \\ \vdots \qquad\qquad \vdots \qquad\qquad \vdots \\ U_1(j\omega_i)G_{q1}(j\omega_i) + \ldots + U_p(j\omega_i)G_{qp}(j\omega_i) &= Y_q(j\omega_i). \end{aligned}$$

This problem can be solved by decomposing it into q MISO problems. In fact, frequency–response data computation of MIMO systems differs from MISO case only in the number of SLE to be solved in each iteration. That is, for each iteration, q SLE are solved rather than just one. As there is no restriction in measuring and considering various input–output channels simultaneously, those q SLE can also be solved simultaneously.

2.4 TFM Identification

Once an FRM has been determined, the second step of the method (Fig. 1) aims to tune a transfer matrix model for the system to be identified.

2.4.1 SISO Case

For the SISO case, the n-order rational transfer function to be estimated, $G_e^n(s)$, can be written as:

$$G_e^n(s) = \frac{N(\underline{\alpha}, s)}{D(\underline{\beta}, s)}, \tag{5}$$

where $N(\underline{\alpha}, s)$ and $D(\underline{\beta}, s)$ are polynomials in s whose coefficients are elements of vectors $\underline{\alpha}$ and $\underline{\beta}$.

Consider the error criterion $J(\underline{\theta})$, based on a quadratic norm, also proposed by Levy (1959) and Sanathanan and Koerner (1963):

$$J(\underline{\theta}) = \left\| D(\underline{\beta}, j\underline{\omega}) \circ G(j\underline{\omega}) - N(\underline{\alpha}, j\underline{\omega}) \right\|_2, \tag{6}$$

where $N(\underline{\alpha}, j\underline{\omega})$ and $D(\underline{\beta}, j\underline{\omega})$ are the frequency responses of numerator and denominator of the model $G_e^n(s)$, respectively, symbol $\circ$ means Hadamard product or element-by-element multiplication, and $\underline{\theta} = [\underline{\alpha}^T \quad \underline{\beta}^T]^{\mathrm{T}}$ is the parameter vector to be determined. Given the frequency response $G(j\underline{\omega})$, the goal is to tune the function $G_e^n(j\underline{\omega})$ by minimizing criterion (6) through $\underline{\alpha}$ and $\underline{\beta}$.

The idea is to determine the model $G_e^n(s)$ as a linear combination of functions of the form presented in (7) and (8), which consider both strictly proper and biproper rational functions possibly having multiple complex poles:

$$G_e^n(\underline{\theta}, s) = \sum_{i=0}^{n} \alpha_i P_i(s) = \frac{N(\underline{\alpha}, s)}{D(\underline{\beta}, s)}, = \frac{\alpha_0 s^n + \alpha_1 s^{n-1} + \cdots + \alpha_{n-1} s + \alpha_n}{\beta_0 s^n + \beta_1 s^{n-1} + \cdots + \beta_{n-1} s + \beta_n}, \tag{7}$$

where:

$$P_i(s) = \frac{s^{n-i}}{\beta_0 s^n + \beta_1 s^{n-1} + \cdots + \beta_{n-1} s + \beta_n}, \tag{8}$$

$$\underline{\alpha} = \begin{bmatrix} \alpha_0 \ \alpha_1 \ \ldots \ \alpha_n \end{bmatrix}^{\mathrm{T}} \in \mathbb{R}^{n+1}, \tag{9}$$

$$\underline{\beta} = \begin{bmatrix} \beta_1 \ \beta_2 \ \ldots \ \beta_n \end{bmatrix}^{\mathrm{T}} \in \mathbb{R}^{n}, \tag{10}$$

$$\underline{\theta} = \begin{bmatrix} \underline{\alpha}^T \ \underline{\beta}^T \end{bmatrix}^{\mathrm{T}} = \begin{bmatrix} \theta_1 \ \theta_2 \ldots \theta_{2n+1} \end{bmatrix}^{\mathrm{T}} \in \mathbb{R}^{2n+1}. \tag{11}$$

For the sake of simplicity, denominator coefficient of term s^n is chosen $\beta_0 = 1$ without loss of generality. For an arbitrarily chosen order n, the following problem of optimization is defined, where $\underline{\theta} \in \mathbb{R}^{2n+1}$:

$$\min_{\underline{\theta}} J(\underline{\theta}) = \min_{\underline{\alpha}, \underline{\beta}} \left\| D(\underline{\beta}, j\underline{\omega}) \circ G(j\underline{\omega}) - N(\underline{\alpha}, j\underline{\omega}) \right\|_2. \tag{12}$$

Function $J(\underline{\theta})$ in (12) is convex, as shown in *Lemma* 1 and hence has a single minimum point (Bazaraa et al. 2006). *Theorem* 1 shows how to compute the optimal solution of the problem in (12).

Lemma 1 $J(\underline{\theta}) : \mathbb{R}^{2n+1} \longmapsto \mathbb{R}$ is convex in $\underline{\theta}$.

Given an n-order approximation of the expansion of $G_e^n(\underline{\theta}, s)$, *then the function* $(J(\underline{\theta}) = \|D(\underline{\beta}, j\underline{\omega}) \circ G(j\underline{\omega}) - N(\underline{\alpha}, j\underline{\omega})\|_2)$ *is convex in the parameter vector* $\underline{\theta} = [\underline{\alpha}^T \ \underline{\beta}^T]^{\mathrm{T}}$.

Proof $J(\underline{\theta})$ is convex in $\underline{\theta}$ if and only if its domain is convex and, for any two points, $\underline{\theta}_1$ and $\underline{\theta}_2$, belonging to it, the following sentence is true $\forall \delta \in [0, 1]$

$$J(\delta\underline{\theta}_1 + (1-\delta)\underline{\theta}_2) \leq \delta J(\underline{\theta}_1) + (1-\delta) J(\underline{\theta}_2). \tag{13}$$

As the domain $\mathbb{R}^{2n+1}$ of $J(\underline{\theta})$ is convex, it remains to demonstrate the inequality (13) is true. Starting from:

$$N(j\underline{\omega}) = \sum_{k=0}^{n} \alpha_k (j\underline{\omega})^{n-k},$$

$$D(j\underline{\omega}) = \sum_{k=0}^{n} \beta_k (j\underline{\omega})^{n-k},$$

$\beta_0 \triangleq 1$, it is possible to write

$$\begin{aligned}
&J(\delta\underline{\theta}_1 + (1-\delta)\underline{\theta}_2) = \\
&= \left\| \left\{ \sum_{k=0}^{n} \left[\delta\beta_{1k} + (1-\delta)\beta_{2k} \right] (j\underline{\omega})^{n-k} \right\} \circ G(j\underline{\omega}) \right. \\
&\quad \left. - \sum_{k=0}^{n} \left[\delta\alpha_{1k} + (1-\delta)\alpha_{2k} \right] (j\underline{\omega})^{n-k} \right\|_2 \\
&= \left\| \delta \left[\sum_{k=0}^{n} \beta_{1k} (j\underline{\omega})^{n-k} \circ G(j\underline{\omega}) - \sum_{k=0}^{n} \alpha_{1k} (j\underline{\omega})^{n-k} \right] \right. \\
&\quad \left. + (1-\delta) \left[\sum_{k=0}^{n} \beta_{2k} (j\underline{\omega})^{n-k} \circ G(j\underline{\omega}) - \sum_{k=0}^{n} \alpha_{2k} (j\underline{\omega})^{n-k} \right] \right\|_2 \\
&\leq \delta \left\| \left[\sum_{k=0}^{n} \beta_{1k} (j\underline{\omega})^{n-k} \circ G(j\underline{\omega}) - \sum_{k=0}^{n} \alpha_{1k} (j\underline{\omega})^{n-k} \right] \right\|_2 \\
&\quad + (1-\delta) \left\| \left[\sum_{k=0}^{n} \beta_{2k} (j\underline{\omega})^{n-k} \circ G(j\underline{\omega}) - \sum_{k=0}^{n} \alpha_{2k} (j\underline{\omega})^{n-k} \right] \right\|_2 \\
&= \delta J(\underline{\theta}_1) + (1-\delta) J(\underline{\theta}_2).
\end{aligned}$$

Theorem 1 *The optimal solution of the problem defined by* (12) *can be determined by solving the following system of linear equations:*

$$\begin{bmatrix} Q_1 & Q_2 \\ Q_3 & Q_4 \end{bmatrix} \begin{bmatrix} \underline{\alpha} \\ \underline{\beta} \end{bmatrix} = \begin{bmatrix} \underline{\mathcal{Y}}_1 \\ \underline{\mathcal{Y}}_2 \end{bmatrix} \tag{14}$$

where $Q_j = \sum_{i=1}^{m} Re[M_j]$, $j \in \{1, 2, 3, 4\}$, $\underline{\mathcal{Y}}_1 = \sum_{i=1}^{m} Re[A]$ *and* $\underline{\mathcal{Y}}_2 = \sum_{i=1}^{m} Re[B]$, *with:*

$$M_1 = \begin{bmatrix} R_n R_n^* & R_n R_{n-1}^* & \ldots & R_n R_0^* \\ R_{n-1} R_n^* & R_{n-1} R_{n-1}^* & \ldots & R_{n-1} R_0^* \\ \vdots & \vdots & & \vdots \\ R_0 R_n^* & R_0 R_{n-1}^* & \ldots & R_0 R_0^* \end{bmatrix},$$

$$M_2 = -M_1(:, 2 : n+1) G^*,$$

$$M_3 = M_1(2 : n+1, :) G,$$

$$M_4 = -M_1(2 : n+1, 2 : n+1) G^* G,$$

$$A = \begin{bmatrix} R_n R_n^* G^* \\ R_{n-1} R_n^* G^* \\ \vdots \\ R_0 R_n^* G^* \end{bmatrix}, \quad B = \begin{bmatrix} R_{n-1} R_n^* G^* G \\ R_{n-2} R_n^* G^* G \\ \vdots \\ R_0 R_n^* G^* G \end{bmatrix}.$$

Terms $M_1(:, 2:n+1)$ and $M_1(2:n+1, :)$ are submatrices of matrix M_1 excluding the first column and the first row, respectively. Dependences on $j\omega_i$, $i \in \{1, 2, \ldots, m\}$, were omitted for the sake of simplicity. Besides, $R_k = R_k(j\omega_i) \triangleq (j\omega_i)^k$, $k \in \{0, 1, \ldots, n\}$.

Proof From (12):

$$J^2(\underline{\theta}) = \sum_{i=1}^{m} \left| D(\underline{\beta}, j\omega_i) G(j\omega_i) - N(\underline{\alpha}, j\omega_i) \right|^2 = \sum_{i=1}^{m} \Psi(j\omega_i) \Psi^*(j\omega_i), \tag{15}$$

with $\Psi(j\omega_i) = D(\underline{\beta}, j\omega_i) G(j\omega_i) - N(\underline{\alpha}, j\omega_i)$.

The optimal solution of the problem in (12) can be determined by means of the following condition:

$$\nabla J^2(\underline{\theta}) = \left(\frac{\partial J^2}{\partial \alpha_0}, \frac{\partial J^2}{\partial \alpha_1}, \ldots, \frac{\partial J^2}{\partial \alpha_n}, \frac{\partial J^2}{\partial \beta_1}, \ldots, \frac{\partial J^2}{\partial \beta_n} \right)^{\mathrm{T}} = [0\ 0\ \ldots\ 0]^{\mathrm{T}}. \tag{16}$$

Note that, as $J(\theta) \geq 0$, the optimal solution for $\min J(\underline{\theta})$ is the same as $\min J^2(\underline{\theta})$. Therefore, partially differentiating (15) with respect to $\underline{\theta}$ in (11):

$$\frac{\partial J^2}{\partial \theta_p} = \sum_{i=1}^{m} \left(\frac{\partial \Psi(j\omega_i)}{\partial \theta_p} \Psi^*(j\omega_i) + \Psi(j\omega_i) \frac{\partial \Psi^*(j\omega_i)}{\partial \theta_p} \right), \tag{17}$$

$$\text{where: } \begin{aligned} \tfrac{\partial \Psi(j\omega_i)}{\partial \alpha_k} &= -(j\omega_i)^{n-k} \triangleq -R_{n-k}, \\ \tfrac{\partial \Psi(j\omega_i)}{\partial \beta_l} &= (j\omega_i)^{n-l} G(j\omega_i) \triangleq R_{n-l} G, \end{aligned} \tag{18}$$

with $k \in \{0, 1, \ldots, n\}$, $l \in \{1, 2, \ldots, n\}$ and R_n and G being functions of $(j\omega_i)$.

Substituting (18) into (17), considering (16) and performing some algebraic manipulations, yields:

$$\frac{\partial J^2}{\partial \alpha_k} = \sum_{i=1}^{m} 2Re[R_{n-k}(j\omega_i) N^*(\underline{\alpha}, j\omega_i) + -R_{n-k}(j\omega_i) G^*(j\omega_i) D^*(\underline{\beta}, j\omega_i)] = 0, \tag{19}$$

$$\frac{\partial J^2}{\partial \beta_l} = \sum_{i=1}^{m} 2Re[R_{n-l}(j\omega_i) G(j\omega_i) N^*(\underline{\alpha}, j\omega_i) + -R_{n-l}(j\omega_i) G(j\omega_i) G^*(j\omega_i) D^*(\underline{\beta}, j\omega_i)] = 0, \tag{20}$$

where $Re[\,.\,]$ represents the real part of the argument. By making some algebraic manipulations in (19) and (20), one can obtain a set of linear equations of the form $Q\underline{\theta} = \underline{\mathcal{Y}}$, as in (14), where the independent term is that corresponding to the coefficient $\beta_0 = 1$. □

2.4.2 MIMO Case

The proposed method for SISO systems can be used successively for each MIMO system channel to obtain a TFM. Alternatively, a joint approach is proposed in this section which considers a common denominator for all channels, whose advantage is a reduced order model with a fewer number of parameters.

For multivariable problems, we redefine the criterion (12), as follows:

$$J(\underline{\theta}) = \sum_{\lambda} \left\| D(\underline{\beta}, j\underline{\omega}) \circ G^{\lambda}(j\underline{\omega}) - N(\underline{\alpha}^{\lambda}, j\underline{\omega}) \right\|_2^2 \tag{21}$$

where $N(\underline{\alpha}^{\lambda}, j\underline{\omega})$, $D(\underline{\beta}, j\underline{\omega})$ are the frequency responses, respectively, of the numerator of λ^{th} channel $G_e^{n,\lambda}(s)$ and of the common denominator of $G_e^n(s)$; and $\underline{\theta} = [\,\underline{\alpha}^{\lambda^T}\ \underline{\beta}^T\,]^{\mathrm{T}}$ is the parameter vector to be determined.

The identification problem for the MIMO case can then be stated as the following optimization problem:

$$\min_{\underline{\theta}} J(\underline{\theta}) = \min_{\underline{\theta}} \sum_{\lambda} \left\| D(\underline{\beta}, j\underline{\omega}) \circ G^{\lambda}(j\underline{\omega}) - N(\underline{\alpha}^{\lambda}, j\underline{\omega}) \right\|_2^2 \tag{22}$$

where $\underline{\theta} = [\underline{\alpha}^{\lambda^T} \underline{\beta}^T]^{\mathrm{T}} \in \mathbb{R}^{q(n+1)p+n}$ e $G^{\lambda}(j\underline{\omega})$ is the frequency response obtained for channel λ.

Following similar steps established for SISO cases, one can obtain:

$$\begin{bmatrix} Q_1 & 0 & \ldots & 0 & -Q_2^{11} \\ 0 & Q_1 & \ldots & 0 & -Q_2^{21} \\ \vdots & & \ddots & \vdots & \vdots \\ 0 & 0 & \ldots & Q_1 & -Q_2^{qp} \\ Q_3^{1\mathrm{T}} & Q_3^{2\mathrm{T}} & \ldots & Q_3^{qp} & -Q_4 \end{bmatrix} \begin{bmatrix} \underline{\alpha}^{11} \\ \underline{\alpha}^{21} \\ \vdots \\ \underline{\alpha}^{qp} \\ \underline{\beta} \end{bmatrix} = \begin{bmatrix} \underline{\mathcal{Y}}_{\alpha}^{11} \\ \underline{\mathcal{Y}}_{\alpha}^{21} \\ \vdots \\ \underline{\mathcal{Y}}_{\alpha}^{qp} \\ \underline{\mathcal{Y}}_{\beta} \end{bmatrix}, \tag{23}$$

where submatrices Q_1 and "0" have the same dimension. Matrices Q_1, Q_2^{λ}, Q_3^{λ} and $\underline{\mathcal{Y}}_{\alpha}^{\lambda}$ have similar structures of Q_j in (14).

3 Numerical Examples

Four numerical applications of the proposed method are presented. The first highlights important properties of FRM computation method in Algorithm 1 when signal are noisy. The second example is intended to simulate the application

of the proposed general algorithm (Fig. 1), notably the steps described in Sects. 2.3 and 2.4 . To identify a MIMO system model, random inputs supposedly not user-manipulable were considered. With the same objective, in third example, we apply overall proposed algorithm to a two-degree-of-freedom (2DOF) Helicopter. Last example consists in applying the method introduced in Sect. 2.4.2 on a MIMO system model of an air–air missile imposing a common denominator in all channels. The following system error criteria is used to evaluate identified models:

$$J = \left\| G(j\underline{\omega})^{\lambda} - G_e^{n,\lambda}(j\underline{\omega}) \right\|_2 . \tag{24}$$

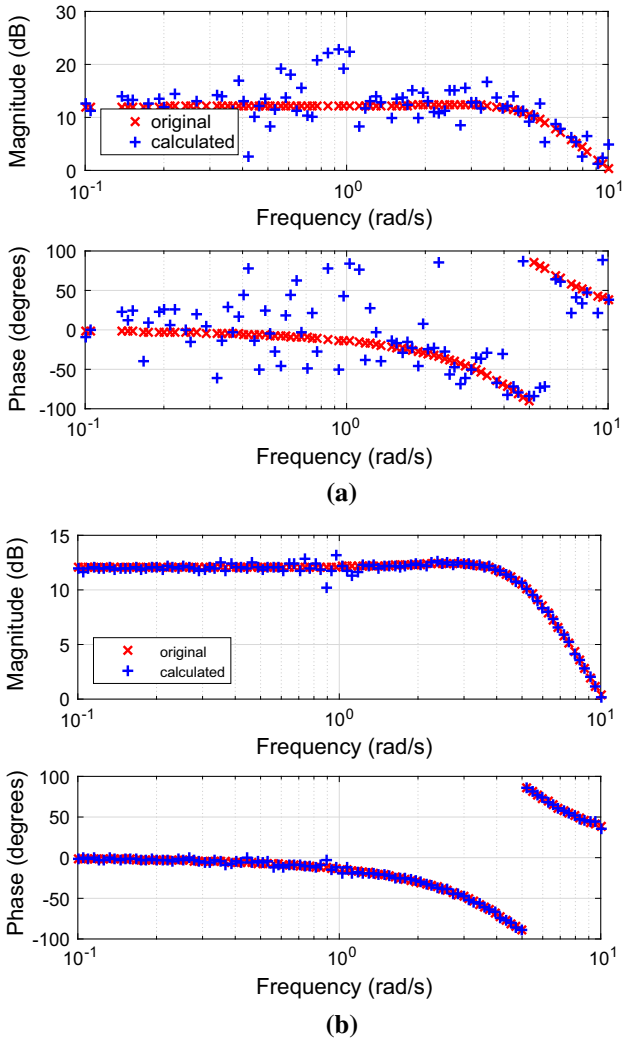

Fig. 5 Frequency response diagram of $G_{13}(s)$ with noise. **a** 1 iteration, **b** 500 iterations

3.1 Example 1

To illustrate the iterative frequency response computation (steps 6 to 7 of the algorithm in Fig. 3), consider the following three-inputs one-output system:

$$G(s) = \left[\frac{4}{s^2+0.2s+1} \;\; \frac{s+5}{s+0.5} \;\; \frac{100}{s^2+6s+25} \right]. \tag{25}$$

A set of input spectra was arbitrarily generated and contaminated with a zero mean noise, uniformly distributed such that the module varied up to 1%. A corresponding set of output spectra was then computed by using (2) and (25). Figure 5 shows the results for channel $G_{13}(j\omega)$ for one (Fig. 5a) and 500 (Fig. 5b) iterations. Frequency response result for one iteration is noisy and not appropriate to be used in the identification phase (Sect. 2.4). Nevertheless, after 500 iterations, the result improved significantly, in spite of some dispersions around 1 rad/s due to the amplification effect associated to the complex pole in channel G_{11} and relative differences of the values between channels. This dispersion can be attenuated or even eliminated by increasing the number of iterations.

3.2 Example 2

The original TFM of this system example is given by (26). Input signals were generated from the sum of rectangular pulses whose amplitudes and widths vary randomly in time. Actuator and sensor noises were considered Gaussian and white with a signal/noise ratio of 20 dB. Input/output data were split into a family of discrete-time windows (Step 2 of Algorithm 1) of 500-s time interval. Each iteration used two windows to obtain a determinate SLE. Maximum number of iterations was chosen as 1000. Table 1 shows the system model errors (24) for all models obtained for this example, for each system channel. Considering that a good model involves both lowest cost and mathematical complexity (order) and, in general, that these criteria tend to be conflicting, one can choose orders corresponding to bold values in Table 1 for each identified model channel. To validate the identified model in time-domain, system responses to random inputs are compared in Fig. 6.

Table 1 System model errors for Example 2

Order	$G_{11}(s)$	$G_{12}(s)$	$G_{21}(s)$	$G_{22}(s)$
1	4.8842	5.7323	0.8053	4.2295
2	**0.8634**	**0.3614**	**0.2472**	0.9003
3	1.5802	0.8759	0.2987	**0.2952**
4	0.9962	0.4709	0.2679	0.4111
5	1.4820	1.0775	0.2800	0.2506

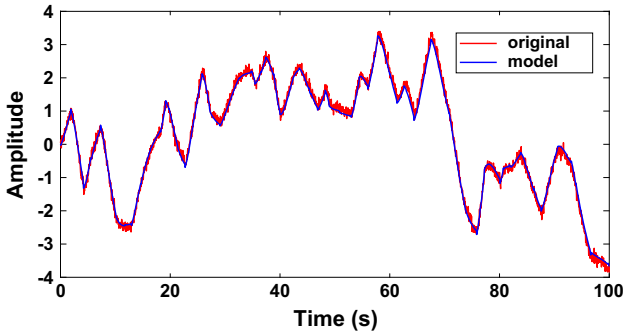

Fig. 6 Time responses (output $y_2(t)$) for original and identified models—Example 2

$$G(s) = \begin{bmatrix} \frac{1}{(s+1)^5} & \frac{1-1.4s}{(s+1)^3} \\ \frac{2(0.5s+1)e^{-0.1s}}{(s+1)(4s+1)} & \frac{1}{(2s+1)^4} \end{bmatrix} \tag{26}$$

The identified TFM $G_e(s)$ is:

$$\begin{bmatrix} \frac{0.1291s^2-0.1535s+0.1693}{s^2+0.5324+0.1550} & \frac{0.2074s^2-0.6861s+0.4073}{s^2+1.0709s+0.4394} \\ \frac{-0.0236s^2+0.1927s+0.4875}{s^2+1.2143s+0.2532} & \frac{-0.0149s^3+0.0132s^2-0.0382s+0.0494}{s^3+0.9166s^2+0.3931s+0.0526} \end{bmatrix} \tag{27}$$

3.3 Example 3—2DOF Helicopter

This example consists of a real plant, the Quanser 2DOF Helicopter (Quanser 2009). The two input reference angles (yaw and pitch) were excited and only the pitch angle output was measured for identification purposes. Only one operating point was taken into account corresponding to zero degree in the two inputs. Since, for this case, the controller engineer is allowed to manipulate the inputs, traditional approach was initially applied for comparison purposes, by introducing a sinusoidal signal in each input at a time. Then, 22 different frequency values ranging between 0.125 rad/s and 18 rad/s were used to excite the system to establish input amplitudes such that neither nonlinearities were excited nor inadequate signal-to-noise ratios were obtained.

Once adequate ranges of amplitudes were defined, sinusoidal signals were simultaneously introduced to both inputs to obtain the FRM and an identified model by using the proposed method. Six different values of amplitudes were used for the inputs at each selected frequency. The number of iterations in Step 6 of Algorithm 1 was set as 1750, were 730 iterations considered three pages and 1020 considered two pages of same data set. Also, for each input frequency value, a different size of time window were used to deal with the balance between dynamic range vs random error. In fact, this property of windowing methods is classical (Tischler and Remple 2012). Time window size selection requires that a compromise be made to improve the accuracy of the frequency response at some frequencies at the expense of other frequencies. The use of larger window size lowers the effective minimum frequency of identification, yielding data at lower frequencies of interest. However, increasing the time windows size reduces the number of frequency-history averages (Step 7) and thereby increases the random error. In contrast, the use of smaller windows results in the opposite trade-off. Then a better identification quality is obtained by using larger windows for low frequencies and smaller windows for high frequencies.

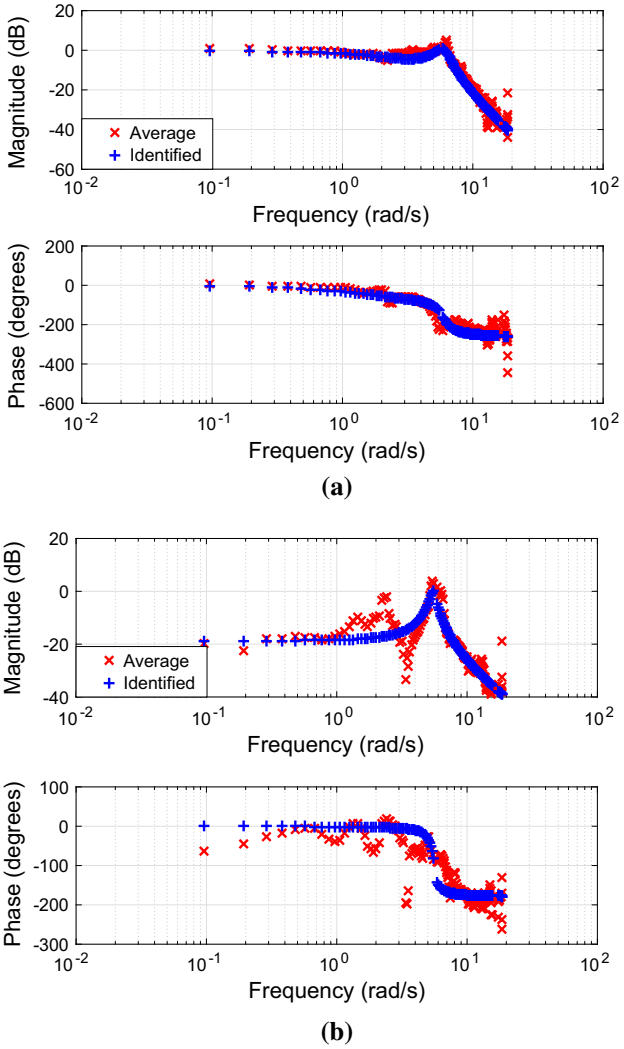

Fig. 7 Calculated frequency response and identified model—Example 3. **a** Channel $G_{11}(j\omega)$, **b** channel $G_{12}(j\omega)$

After determining the FRM average (Step 7), the identification method proposed in Sect. 2.4 can be performed. Fig. 7 displays the computed average FR of measured data and of the corresponding identified model data. Considering a cost criterion and the model complexity involved, the model order for the first channel, $G_{11}(s)$, and for the second channel, $G_{12}(s)$, were selected as 3 and 2, respectively. Although

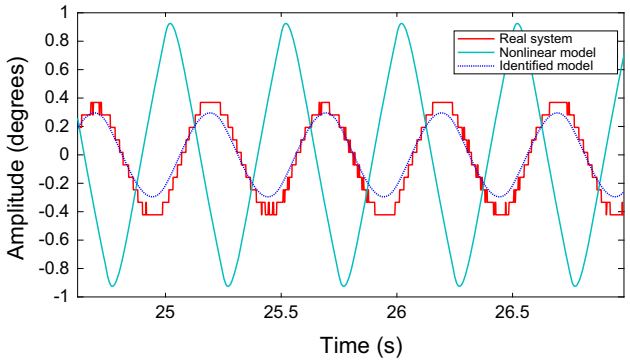

Fig. 8 Response to square wave inputs—Example 3

channel $G_{12}(s)$ appears to be poorly tuned, it should be noted that, in low frequencies, its magnitude is 20 dB more attenuated than that of the other channel and the excursion of inputs is limited in amplitude for practical reasons. These facts allow us to apply the principle of parsimony by adopting a lower order for $G_{12}(s)$, which did not lead to a good frequency fitting for this channel but has been proven effective in the time domain as shown by results in Fig. 8.

In order to validate the identified model, the real closed-loop system, the nonlinear closed-loop model in (Quanser 2009) and the identified model were submitted to the same inputs which are different from those used for identification purpose. Figure 8 presents responses to square wave inputs. Different input amplitudes were used for each channel. The identified model behavior is closer to that of the real system. Despite the relatively low order chosen for the identified model, its time-domain output behavior adequately represents the system dynamics. Similar results were found by using chirp function inputs.

3.4 Example 4—Air-to-Air Missile

In this example, the application of MIMO identification technique presented in Sect. 2.4.2 is illustrated for the case where each transfer function has a common denominator. The air-to-air missile model presented in (Reichert 1992; Nichols et al. 1993) is studied. The nonlinear pitch-axis missile model represents a missile flying at an altitude of 20,000 feet at Mach 3. The input is the commanded tail fin deflection, and measured outputs are the normal acceleration and the pitch rate. A fourth-order linearized model representing the missile and actuator was obtained from the first-order Taylor expansion around the operating condition determined by the angle of attack equal to 15 degrees. This model was used to generate the frequency response data corresponding to 100 values of frequency uniformly log-spaced, in a range of 0.01 rad/s to 100 rad/s. Obtained costs are summarized in Table 2 and FR of channel $G_{21}(s)$ are depicted in Fig. 9. These results show that a third-order tuned model can represent the original model dynamics with a good precision. Table 3 shows the coefficients of the identified fourth-order model.

Table 2 System model errors for Example 4

Ord $D(s)$	Cost/channel (J_λ)		Total cost
	1:1	2:1	$(J_M = \sum J_\lambda)$
2	8.1467	30.5079	38.6545
3	0.7709	2.7901	3.5611
4	2.429×10^{-11}	3.911×10^{-11}	6.3402×10^{-11}
5	1.319×10^{-11}	2.235×10^{-11}	3.555×10^{-11}

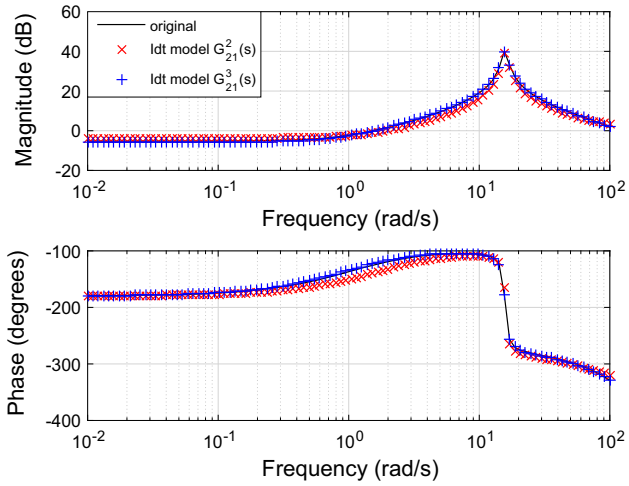

Fig. 9 Frequency responses of channel 2:1: identified models ($G_e^2(s)$ and $G_e^3(s)$) and original model $G(s)$

Table 3 Coefficients of $G_e^4(s)$ for Example 4

Term	Numerator		Denominator
	1:1	2:1	
s^4	0.00000	0.00000	$+1.0000$
s^3	0.00000	0.00000	$+2.1126 \times 10^2$
s^2	-4.5849×10^3	0.00000	$+2.3011 \times 10^4$
s^1	$+2.8318 \times 10^2$	-2.9445×10^6	$+8.0136 \times 10^4$
s^0	$+5.6365 \times 10^6$	-3.0488×10^6	$+5.5584 \times 10^6$

4 Conclusion

The method proposed in this paper is suitable for the multivariable system identification. Identified models are based on FRM computed from the time input–output signals which can be also measured during the normal system operation, possibly without the need of introducing special classes of input signals. In this case, effectiveness of the method depends on

how rich data measurements are with respect to information about system dynamics in the frequency spectrum range of interest.

In principle, once the time data are measured and stored, we consider offline applications for our method. While the first step of the algorithm (obtaining the frequency response) can be implemented recursively, the second one (MFT Identification) cannot be. Given an estimated model order, the solution in the latter is directly computed based on the frequency response found in the former. Also, the frequency response computed in the first step improves as new data are considered at each iteration.

For MIMO cases, all channels of identified models share the same dynamics, i.e., they have the same set of poles. Once FRM is obtained, rational and proper transfer function models are estimated by computing a sequence of optimal and analytical solutions to a convex problem based on a quadratic criterion. Models are chosen considering a trade-off between small cost and low complexity (small order).

Computational implementations are relatively simple, involving, in general, matrix computations. Numerical examples evidenced some advantages and limitations of the proposed method. Proposed procedure obtains good results in few iterations, in cases where input–output data are noise free. Contrarily, when signals are noisy, the increase in number of iterations works as a filtering process by computing frequency response averages. This strategy allows this deterministic method to treat stochastic signals. Finally, results from the application of proposed method on a 2DOF helicopter demonstrated its effectiveness in identifying linear models for real systems where nonlinearities and noises are present.

References

Akçay, H., & Heuberger, P. (2001). A frequency-domain iterative identification algorithm using general orthonormal basis functions. *Automatica*, *37*(5), 663–674.

Bazaraa, M. S., Sherali, H. D., & Shetty, C. M. (2006). *Nonlinear programming theory and algorithms* (3rd ed.). New York: Wiley.

Bossa, T. H. S., Martins, N., da Silva, R. J. G. C., & Pellanda, P. C. (2011). A field test to determine PSS effectiveness at multigenerator power plants. *IEEE Transactions on Power Systems*, *26*(3), 1522–1533.

Drmac, Z., Gugercin, S., & Beattie, C. (2015). Vector fitting for matrix-valued rational approximation. *SIAM Journal on Scientific Computing*, *37*(5), 2151–5626.

Galrinho, M. (2016). Least squares methods for system identification of structured models. Ph.D. thesis, KTH School of Electrical Engineering.

Levy, E. C. (1959). Complex-curve fitting. *IRE Transactions on Automatic Control*, *AC–4*(1), 37–43.

Ljung, L. (1999). *System identification: Theory for the user* (2nd ed.). New York: Prentice Hall.

Ljung, L. (2013). Some classical and some new ideas for identification of linear systems. *Journal of Control, Automation and Electrical Systems*, *24*, 3–10.

Militaru, R., & Popa, I. (2012). On the numerical solving of complex linear systems. *International Journal of Pure and Applied Mathematics*, *76*(1), 113–122.

Nichols, R., Reichert, R., & Rugh, W. (1993). Gain scheduling for H-infinity controllers: A flight control example. *IEEE Transactions on Control Systems Technology*, *1*(2), 69–79.

Ninness, B. (1996). Frequency domain estimation using orthonormal bases. In: Proceedings of 13th world congress. San Francisco, USA: IFAC.

Ninness, B. (1998). A stochastic approach to linear estimation in H_∞. *Automatica*, *34*(4), 405–414.

Oliveira, G. H. C., Rosa, A., Campello, R. J. G. B., Machado, J. B., & Amaral, W. C. (2011). An introduction to models based on laguerre, kautz and other related orthonormal functions-part I: Linear and uncertain models. *International Journal of Modelling, Identification and Control*, *14*(1/2), 121–132.

Oliveira, M.A., Ades, R., & Pellanda, P. C. (2017). Método iterativo de identificação de modelos dinâmicos multivariáveis no domínio da frequência a partir de sinais temporais. In: Simpósio Brasileiro de Automação Inteligente, Brazilian Society of Automatics, (pp. 183–190).

Pintelon, R., & Schoukens, J. (2012). *System identification: A frequency domain approach* (2nd ed.). New York: IEEE.

Quanser. (2009). 2DOF Helicopter Reference Manual.

Reichert, R. (1992). Dynamic scheduling of modern-robust-control autopilot designs for missiles. *IEEE Control Systems Magazine*, *12*(5), 35–42.

Sanathanan, C. K., & Koerner, J. (1963). Transfer function synthesis as a ratio of two complex polynomials. *IEEE Transactions on Automatic Control*, *8*, 56–58.

Schumacher, R., Oliveira, G. H. C., & Mitchell, S. D. (2015). An iterative approach for selecting poles on complex frequency localizing basis function-based models. *Journal of Control, Automation and Electrical Systems*, *26*, 380–389.

Strang, G. (2006). *Linear algebra and its applications* (4th ed.). Boston: Brooks Cole.

Tischler, M. B., & Remple, R. K. (2012). *Aircraft and rotorcraft system identification* (2nd ed.). New York: AIAA.

Tóth, R. (2010). *Modeling and identification of linear parameter-varying systems*., Lecture notes in control and information sciences Berlin: Springer.

Vizer, D. (2015). Application of the H_∞-norm for the identification of linear time-invariant and linear time-varying models. Ph.D. thesis, University of Poitiers.